Journal of Electroceramics, 13, 759–763, 2004
© 2004 Kluwer Academic Publishers. Manufactured in The Netherlands.

Bulk Grain Resistivity of ZnO-Based Varistors

A.C. CABALLERO,[1] D. FERNÁNDEZ HEVIA,[*,2] J. DE FRUTOS,[2] M. PEITEADO[1] & J.F. FERNÁNDEZ[1]

[1]*Dpto. de Electrocerámica, Instituto de Cerámica y Vidrio, CSIC, 28049 Cantoblanco, Madrid, Spain*
[2]*E.T.S.I. Telecomunicación, Univ. Politécnica de Madrid, Ciudad Universitaria s/n, 28040 Madrid, Spain*

Submitted ; Revised ; Accepted

Au: Pls. Provide dates & Keywords.

UNCORRECTED PROOF

Abstract. We study the temperature dependence of grain resistivity in ZnO ceramic varistors (300–430 K), finding a positive temperature coefficient (PTC). We devise a high-frequency procedure that allow us to obtain the concentration and energy position of the shallow donor. The observed behavior is consistent with a shallow donor approaching complete ionization, and with an electron mobility mainly controlled by lattice (both optical and acoustical) scattering. The impact of this behavior on varistor performance under high-current pulse loads is discussed.

Keywords:

1. Introduction

Polycrystalline semiconductors with electrically active interfaces are interesting from the fundamental and technological points of view [1]. Their nonlinear charge transport properties strongly depend upon the electronic structure of the three different microscopic regions within each grain [1–3]. (1) the interface or grain boundary (GB), characterized by the existence of a surface density of states; (2) the depletion layer (DL), characterized by the presence of deep levels, which are usually described by their concentration, energy position, and capture cross section; (3) and, finally, the bulk grain region, characterized by the presence of a shallow donor (responsible for the n-type conductivity of ZnO), which is described by its density N_0 and energy position ξ_0. A correct understanding of bulk-grain-related phenomena is important in ceramic overvoltage protection devices because grain resistivity is closely related to high-field performance [4–6], and in applications of polycrystalline semiconductors as microwave materials [1, 7], because bulk-grain properties control the high frequency response. In the particular case of ZnO, the study of the physics and chemistry of the shallow donor is a very active research topic due to its implications in spintronics [8], transparent conductors, gas sensors, varistors, and optoelectronics [9]. Despite this relevance, bulk grain properties of ceramic semiconductors have not received much attention, and shallow donor spectroscopic techniques based in the analysis of the electrical response of a ceramic sample have not been developed. In the case of ZnO varistors, a few works have been published where suitable electrical measurements directly yield grain resistivity [4, 5], and an infrared reflectance technique [6], was proposed that indirectly measures free-electron density and then converts it into grain resistivity.

In this work, we develop an spectroscopic technique that yields the concentration and thermal activation energy of a shallow donor in the grain interiors of ceramic semiconductors. Then, we present the positive temperature coefficient of resistivity (PTCR) of the bulk grains of ZnO-based varistor ceramics, and discuss its implications on varistor performance under high current pulse loads.

2. Theoretical Background

At zero applied field, the conditions for electrical measurements to yield meaningful information about grain interiors can be understood through the broadband

*To whom all correspondence should be addressed. E-mail: dhevia@fis.upm.es

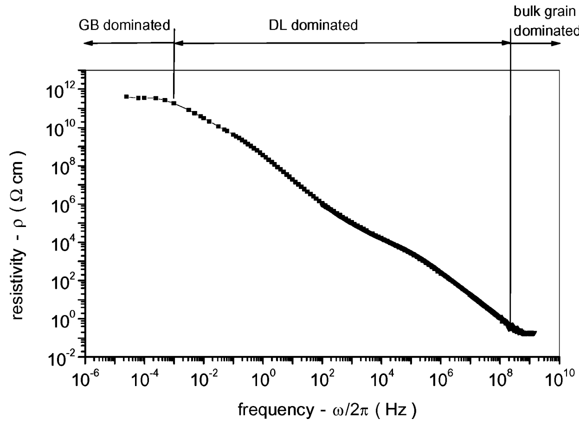

Fig. 1. Series resistivity measured over a very broad spectral range and showing clear convergence at the high-frequency limit, when the interfaces and depletion layers are shorted through the high frecuency capacitance.

electrical response of Fig. 1. Close to the dc limit, charge transport is dominated by thermionically emitted over-barrier currents [1, 2], and the dc resistance presents a well known negative temperature coefficient (NTC) due to the temperature dependence of the thermionic current. Upon increasing frequency, the dielectric response of the material takes control of its electrical properties, and the real part of the impedance becomes a meaningless parameter in itself, devoid of a clear physical meaning, through more than ten orders of magnitude in frequency. Finally, as soon as the capacitance ($C_p = Im(Y^*)/\omega$) of the material converges to its high-frequency value [10], the control of the transport properties moves to the bulk grain region and the bulk grain resistance emerges, turning the system into a series R_G-C_{HF}-L combination. The test for the system to have reached its high frequency limit is the convergence of the real part of the impedance, which has no reason to converge to anything unless the high frequency limit has been actually reached (with the GBs shorted through the high frequency capacitance), in whose case it converges to the grain resistance.

3. Experiment

Up to this point, the discussion is generally valid for any polycrystalline semiconductor. We now focus in ZnO-based varistors. Electrical measurements up to 1 GHz were performed on rod-shaped samples Ø1.5 and 4 mm long, machined to this size in order to delay the onset of the geometrical resonance [5], and to ensure complete penetration of the electromagnetic measuring signal [11, 12]. Samples were taken from commercial-grade, high voltage (3 kV-rated, 3.33 kV/cm residual voltage at 0.8 kA/cm^2) ZnO varistors. R_G values have been converted to $\Omega \times$ cm by using microstructural information about the percentage of secondary phases in a polished, chemically etched cross-section of the varistor material (approximately 6%). The experiments were performed by placing the sample on a radio-frequency commercial bridge, and heating the sample with a computer controlled system. At each temperature, the high-frequency response in the range 10^8–10^9 Hz was recorded and convergence of the series resistivity, such as that shown in Fig. 1, was verified. The bulk grain resistivity of the sample was taken to be that value attained at 1 GHz. Finally, high field measurements were performed on samples of Ø2.5 and 3 cm thick, with the aid of a specifically designed capacitor-bank circuit.

4. Results and Discussion

The experimental points of Fig. 2 constitute our main experimental result. We find a small but well defined positive temperature coefficient (PTC) for the bulk

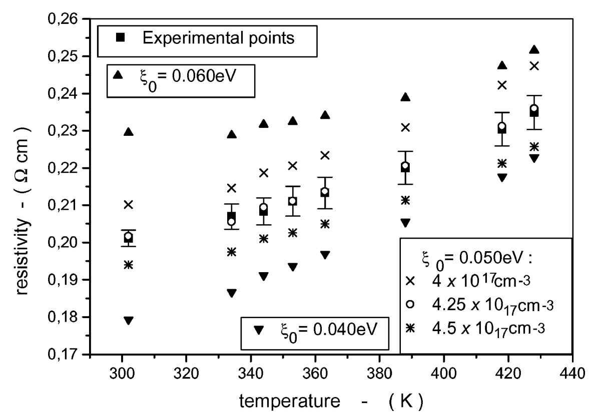

Fig. 2. Bulk PTC behavior in a typical ZnO-based varistor. The figure shows the experimental points, along with calculated curves corresponding to $\xi_0 = 0.05$ eV and three different values of N_0 (the total shallow donor density). Two additional curves correspond to fixed $N_0 = 4.25 \times 10^{17} \text{cm}^{-3}$ and $\xi_0 = 0.04/0.06$ eV.

UNCORRECTED PROOF

grain resistivity: the grain interiors are found to behave in a metallic-like way. To explain this result, we first write the grain resistivity ρ_G as

$$\rho_G = 1/(n\mu e), \tag{1}$$

where n and μ are the free carrier density and mobility in the grains. Before proceeding further, we need to clarify to what extent can we compare our high-frequency ρ_G values, with those calculated from the intrinsically dc Eq. (1). To this end, we use a simplified treatment of charge carrier inertia [13] that has been successfully applied to the high-frequency analysis of GaAs Schottky diodes [14, 15]: free carrier conduction in a semiconductor is represented by a complex conductivity

$$\sigma = \sigma_0/(1 + i\omega\tau) \tag{2}$$

where $\sigma_0 = n\mu e$ is the dc conductivity, $\tau = \mu m^*/e$ is the average free carrier relaxation time [13], and m^* is the free carrier effective mass. Hence, carrier inertia effects are negligible when $\omega\tau \ll 1$; introducing appropriate values for ZnO at room temperature [16–18] ($m^* = 0.27 m_0$ and $\mu = 140$ cm^2/Vs), this condition implies $\omega \ll 4 \times 10^{13}$ Hz. Therefore, the electrical conductivity of bulk ZnO remains very close to its dc value up to the THz range, and we can safely compare our experimental results with the ρ_G values to be calculated through Eq. (1). To do so, we note that reported [16–18] ZnO mobility-vs.-temperature curves for a wide range of doping conditions, converge above room temperature due to the dominance of lattice over impurity scattering. Hence, we can select a reported μ-T curve [18] and, for each temperature, directly introduce the experimental mobility values in Eq. (1). Now, as thermodynamic calculations have shown that room temperature charge balance within varistor ZnO grains is maintained between electrons in the conduction band and ionized shallow donors [19], we can write the charge balance equation as

$$n = N_C e^{-\xi/k_B T} = \frac{N_0}{1 + 2\exp\left[(\xi_0 - \xi)/k_B T\right]}, \tag{3}$$

where n is the free carrier density, N_C is the conduction band effective density of states and ξ is the Fermi level. At each fixed temperature, and assuming a particular value for ξ_0 and N_0 in Eq. (3), we can solve it for ξ and n, therefore calculating the quantity $1/n\mu e$. Hence, corresponding to particular values of ξ_0 and N_0, we can obtain a calculated ρ_G vs. T to be compared with the experimental one. Figure 2 shows how the value of ξ_0 controls the shape of the calculated ρ_G vs. T curve, while N_0 controls its relative height with respect to the vertical axis. For a given experimental ρ_G vs. T curve, one can find only one couple (ξ_0, N_0) that accurately reproduces experiment. The values we have found are $\xi_0 = 0.05$ eV and $N_0 = 4.25 \times 10^{17}$cm^{-3}. The corresponding free carrier density is $n = 2.3 \times 10^{17}$cm^{-3} at room temperature, in agreement with values obtained from reflectance measurements [6]. We then conclude that, at room temperature and above, a shallow donor approaching complete ionization and a lattice-scattering controlled mobility, render a PTC for the bulk-grain resistivity. This PTC feature could explain the results obtained in Ref. 20 by Modine et al., who found that current amplitude decreased with successive current pulse applications: here, the behavior of the sample is bulk-grain dominated due to the barrier-suppressing applied field, and Joule heating of the samples could manifest itself in an increase of grain resistance, leading to currents that decrease for constant applied voltage [20]. This type of behavior is important for varistor stability under typical pulse and multi-pulse current testing, as prescribed by international standards [21]. To obtain independent verification of this high-field PTC behavior, we have performed a series of pulsed-current high field measurements. Samples were subjected to 10^3 A/cm^2 high current pulses in order to drive them as close as possible to the high-field ohmic region of their I-V characteristic [4, 5], without degrading or breaking them. Figure 3(a) presents one such a pulse, to be compared with that of Fig. 3(b), corresponding to a much smaller current density of 25 A/cm^2, which still shows a very clear non-ohmic behavior. Samples were self-

Table 1. Values extracted from the high-field measurements of Fig. 3. Sample temperature increases due to self-heating, and sample resistance increases with sample temperature.

Pulse #	Sample resístance (mΩ)	Surface temperature before/after pulse (K)
1	170 ± 5	300/325
2	187 ± 5	336/349
3	201 ± 5	359/371

UNCORRECTED PROOF

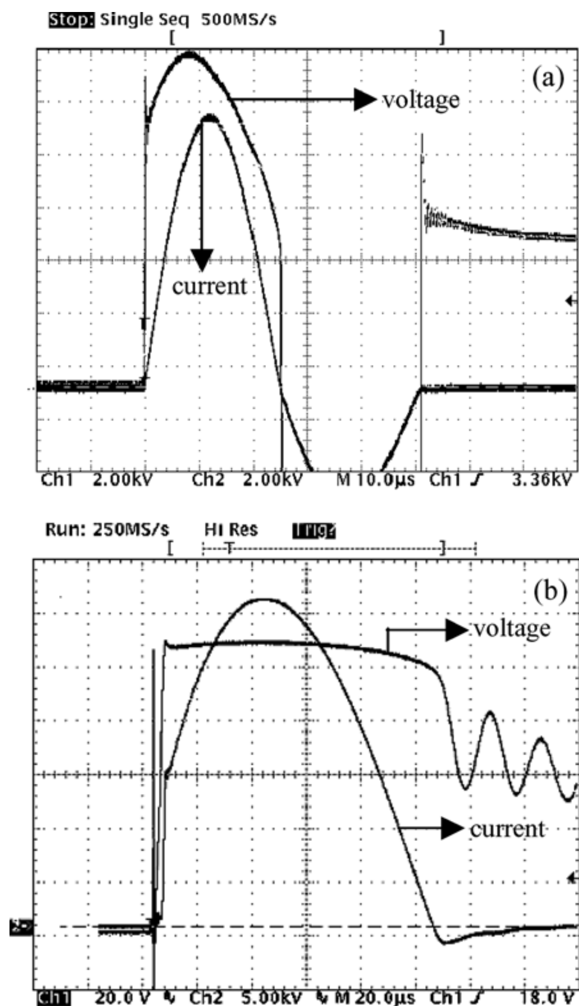

Fig. 3. High field measurements supporting a high field PTC behavior in a typical ZnO-based varistor. Figure 3(a) corresponds to a 20 kA current pulse, with the electrical response approaching a high-field ohmic behavior. Figure 3(b) corresponds to a 500 A current pulse, and the electrical response is clearly non-ohmic.

heated due to high current flow. Surface temperature was recorded 0.5 s before and 0.5 s after each pulse. Table 1 presents the relevant parameters obtained from a sequence of three pulses such as the one in Fig. 3(a), separated by a 3 s lapse. Peak values of the current and voltage traces were used to evaluate sample resistance. Note that reliable resistivity data can not be obtained in the high field regime due to current constriction [5], but the increase of resistance with sample temperature is clear and consistent with the high frequency data.

5. Conclusions

We have devised a technique which allows to obtain the concentration and energy level of the shallow donor in polycrystalline *n*-doped ZnO. As an application, we have shown that ZnO-based varistor materials exhibit a transition from NTC to PTC behavior, as the control of the electrical properties changes from the interface/depletion-layer regions to the bulk grain region. The NTC/PTC cross-over can be defined either by a high enough frequency such that the material reaches its geometrical capacitance, or by an applied field that suppresses the grain boundary electrostatic barriers. We have shown that this PTC behavior explains relevant features of the pulse behavior of varistor devices.

Acknowledgments

We acknowledge support from CICYT, project MAT2001-1682-C02-01/02.

References

1. G.E. Pike, "Semiconducting polycrystalline ceramics," in *Materials Science and Technology*, edited by M.V. Swain (VCH, Weinheim, Germany, 1994), Vol. 11, pp. 731–754 .
2. D. Fernández Hevia, J. de Frutos, A.C. Caballero, and J.F. Fernández, *Appl. Phys. Lett.*, **83**, 2692 (2003).
3. G. Blatter and F. Greuter, *Phys. Rev.*, **B33**(6), 3952 (1986).
4. W.G. Carlson and T.K. Gupta, *J. Appl. Phys.*, **53**(8), 5746 (1982).
5. L.M. Levinson and H.R. Phillipp, *J. Appl. Phys.*, **47**(7), 3116 (1976).
6. H.R. Phillipp and L.M. Levinson, *J. Appl. Phys.*, **47**(3), 1112 (1976).
7. N. McN. Alford, S.J. Penn, A. Templeton, X. Wang, and S. Webb, *Industrial Ceramics*, 21(1), **21** (2001).
8. T. Fukumura, Z. Jin, A. Ohtomo, H. Koinuma, and M. Kawasaki, *Appl. Phys. Lett.*, **75**, 3366 (1999).
9. D.C. Look, *Mater. Sci. Eng. B*, **80**(1–3), 383 (2001).
10. D. Fernández-Hevia, J. de Frutos, A.C. Caballero and J. F. Fernández, *J. Appl. Phys.*, **92**(5), 2890 (2002).
11. I.M. Kaganova and M.I. Kaganov, *Phys. Lett. A*, **173**, 473 (1993).
12. A. Rinkevich, A. Nossov, V. Ustinov, V. Vassiliev, and S. Petukhov, *J. Appl. Phys.*, **91**(6), 3693 (2002).
13. K.S. Champlin, D.E. Armstrong, and P. D. Gunderson, *Proc. IEEE*, **52**, 677 (1964).
14. O.V. Roos and K.L. Wang, *IEEE Trans. Microwave Theory Tech.*, **MTT-34** (1), 183 (1986).
15. U.V. Bhapkar and T.W. Crowe, *IEEE Trans. Microwave Theory Tech.*, **MTT-40**(5), 886 (1992).

UNCORRECTED PROOF

247 248 249 250 251 252

16. A.R. Hutson, *Phys. Rev.*, **108**(2), 222 (1957).
17. K.I. Hagemark and L.C. Chacka, *J. Solid State Chem.*, **15**, 261 (1975).
18. E. Ziegler, A. Heinrich, H. Oppermann, and G. Stöver, *Phys. Stat. Sol.* (a) **66**, 635 (1981).
19. G.D. Mahan, *J. Appl. Phys.*, **54**(7), 3825 (1983).
20. F.A. Modine and R.B. Wheeler, *J. Appl. Phys.*, **67**(10), 6560 (1990).
21. International Electrotechnical Comission, Std. IEC 60099-4, *Surge Arresters Without Gaps* (1998); ANSI/IEEE Std. C62.11, *IEEE Standard for Metal-Oxide Surge Arresters for Alternating Current Power Circuits* (1993).

253 254 255 256 257 258

UNCORRECTED PROOF